J Sol-Gel Sci Technol (2017) 83:447–456
DOI 10.1007/s10971-017-4424-x

ORIGINAL PAPER: SOL-GEL AND HYBRID MATERIALS FOR OPTICAL, PHOTONIC AND OPTOELECTRONIC APPLICATIONS

Synthesis and luminescent properties of monodisperse SiO_2@SiO_2: Eu(DBM)$_3$phen microspheres with core-shell structure by sol–gel method

Yongren Mou[1] · Ming Kang[1] · Feng Wang[1] · Min Liu[1] · Kexu Chen[1] · Rong Sun[1]

Received: 18 January 2017 / Accepted: 13 May 2017 / Published online: 25 May 2017

Abstract Monodisperse core-shell structured SiO_2@SiO_2: Eu(DBM)$_3$phen microspheres, as a new kind of fluorescent particles, were fabricated by a seeded growth method in the presence of surfactant CTAB (DBM = dibenzoylmethane, phen = 1,10-phenanthroline, CTAB = cetyltrimethyl ammonium bromide). In this way, a thin mesoporous silica shell doped with Eu(DBM)$_3$phen was grown on the prepared monodisperse silica colloids. The structures of the as-prepared phosphors were characterized by means of X-ray diffraction, Fourier transform infrared spectrum, thermal gravimetric analysis–differential scanning calorimetry, field emission scanning electron microscopy, transmission electron microscopy, energy-dispersive X-ray spectrometry, nitrogen adsorption-desorption techniques, and photoluminescence spectra. The experimental results show that the microshpere has a typical core-shell structure with a diameter of about 370 nm, consisting of the silica colloids core with about 340 nm in diameter and mesoporous silica shell doped with europium complexes with an average thickness of about 15 nm. The as-obtained core-shell microspheres exhibit a strong red emission peak originating from electric-dipole transition $^5D_0 \rightarrow {}^7F_2$ (610 nm) of Eu^{3+} ions under the excitation of 405 nm. Additionally, the photoluminescence intensity increases with the increasing of europium complexes concentration in mesoporous silica shell, and concentration quenching occurs when europium complexes concentration exceeds 7.0 mol%. The prepared microspheres may present potential applications in the fields of optoelectronic devices, bio-imaging, medical diagnosis, and the packing structural functional composites.

Graphical Abstract Monodisperse core-shell structured SiO_2@SiO_2: Eu(DBM)$_3$phen microspheres with high lumious performance were fabricated by a seeded growth method by means of surfactant CTAB.

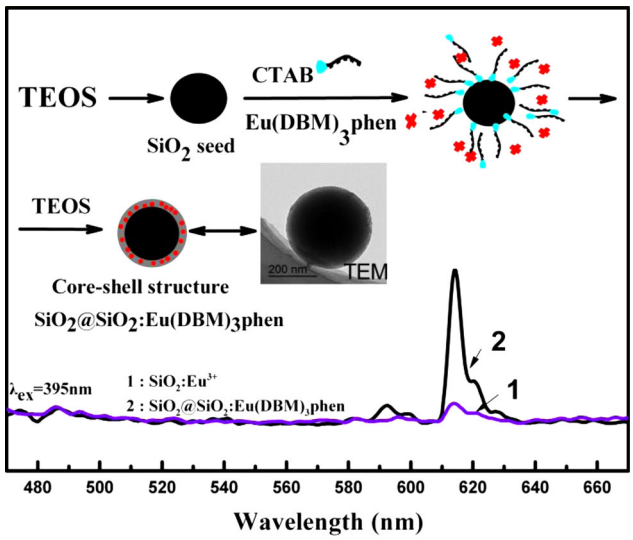

Keywords Core-shell structure · SiO_2@SiO_2:Eu(DBM)$_3$phen microspheres · Seeded growth method · Luminescence · Rear earth complexes

1 Introduction

Rare earth (RE) composite materials played a critical role in the luminescent materials area, having been widely used in

✉ Ming Kang
dyw510@126.com

[1] College of Materials Science and Engineering, Southwest University of Science and Technology, 621010 Mianyang, China

novel photovoltaic materials, display technique, optical detection, and bio-medical imaging [1–5], as a result of their optical, electronic, and chemical features arising from the 4 f electrons of RE ions. For the past decades, a variety of researches have been employed for preparing RE composite materials which are mainly concentrated in the matrix of oxide [6, 7], sulfide [8], aluminate [9], silicate [10], and carbonate [11]. Among all kinds of these phosphors, silica-based fluorescent materials, especially the spherical silica-based phosphors are considered as excellent candidates that provide definite fluorescent emission signals, low light scattering, good photochemical stability and biocompatibility, making them suitable for drug tracing, biological label, display and microscopic analysis of composite materials [12–16]. However, it is difficult to prepare RE-doped monodispersed silica spheres by the traditional sol-gel method. The reason is that RE ions are usually rapidly precipitated in basic environments, leading to lanthanide incorporation inconsistent with silica particles, while the acid-catalyzed hydrolysis of Tetraethyl orthosilicate (TEOS) generally results in uncontrollable with sizes and size distributions of large particles [17]. In recent years, some methods have been utilized to prepare RE-doped silica spheres, Liu et al. [18] obtained europium doped silica microspheres using the W/O microencapsulation method with the assistance of the surfactant 3-aminopropyl-triethoxysilane. Dood et al. [19] and Gong et al. [17] used alkali-catalyzed method to produce uniform sized SiO_2 core, then used acid-catalyzed method to grow SiO_2 shell doped with RE ions in the kernel growth. However, as the low fluorescence intensity of single RE ions doped materials, high doping content of RE ions is needed, which may be limited by the expensive price of RE ions and the occurrence of concentration quenching effect. So it is necessary to replace the RE ions with RE complexes.

RE complexes are ideal optical materials because of their excellent fluorescent radiation, narrow half-peak breadth, high color purity, and large Stockes shift. When the SiO_2 gel was doped with RE complexes, it can not only improve the stability and biocompatibility of the RE complexes but also get high fluorescence intensity [20]. Nevertheless, it is also difficult to get RE complex-doped monodispersed silica spheres by the Stöber method, as the RE complexes colloidal particles are easy to reunite and have poor solubility in the environment of alcohol-water system, which makes it is hard to incorporate the RE complexes into the microspheres. At present, methods for making spherical silica hybrid materials based on RE complexes mainly include chemical immobilization and forming core-shell structure. Zhang et al. [21] immobilized Lanthanide (III)-imidazole dicarboxylic acid complexes on colloidal mesoporous silica with diameter smaller than 100 nm by covalent bond grafting technique and obtained functionalized silica. Zhao et al. [22–24] utilized the solubility difference of RE complexes and composite microspheres in acetone solution and employed the improved Stöber method to get the composite microspheres with core-shell structure. Yu et al. [25] fabricated sphere-shape $Eu(DBM)_3Phen@SiO_2$ nanoparticles by employing a modified alkaline catalyzed hydrolysis and precipitation method and assistance of PVP. However, it is hard to obtain the particles with good sphericity and monodispersity prepared as described above, and the particle size are difficult to be controlled. What's more, it will consume large amounts of Re complexes when it acts as the core of the core-shell composites.

In this paper, we prepared monodisperse spherical silica particles, then a continuous europium complexes-doped mesoporous silica shell was coated on the surface of the silica core via a modified alkaline catalyzed hydrolysis and precipitation method. The core-shell structure monodisperse $SiO_2@SiO_2$:$Eu(DBM)_3$phen microspheres were obtained. The microspheres have the following advantages: (1) the fluorescent signal has been enhanced a lot and photostability has been increased by encapsulating the hydrophobic europium complexes into hydrophilic silica shell by means of surfactant cetyltrimethyl ammonium bromide (CTAB); (2) the particles have good sphericity and homogeneous particle size for the monodisperse silica spheres acting as the seeds; (3) good sphericity and narrow diameter particles have been obtained by a modified sol-gel method in a low doping content of RE complexes which can reduce the cost of the phosphors to some extent; (4) the impact on hydroxyl activity of the surface of SiO_2 for the incorporation of RE complexes has been reduced as far as possible which can keep a high activity for the phosphors. The as-obtained core-shell structured phosphors show much stronger red light emission under ultraviolet light excitation compared with the phosphors doped with single RE ions, and it may have potential applications in the fields of optoelectronic devices, bioimaging, medical diagnosis, and study on the structure of functional composites. Furthermore, the possible formation mechanism of the architecture was discussed in detail.

2 Experimental

2.1 Materials and methods

TEOS, ammonium hydroxide (25 wt%), acetone, Cetyltrimethyl Ammonium Bromide (CTAB), 1,10-phenanthroline (phen) were obtained from Chengdu Kelong Chemical Co, Ltd. $Eu(NO_3)_3{\cdot}6H_2O$ (99.99%) and dibenzoyl methane (DBM) were purchased from Aladdin Reagent Co. All chemicals were analytical grade reagents and used directly without further purification.

2.2 Synthesis of rear earth complexes $Eu(DBM)_3phen$

The RE complexes $Eu(DBM)_3phen$ was synthesized as report [26], 1 mmol $Eu(NO_3)_3$ was dissolved in ethanol to form $Eu(NO_3)_3$ ethanol solution (solution a). 3 mmol dibenzoylmethane (DBM), 1 mmol phen and 1 mmol NaOH were dissolved in ethanol to form settled solution (solution b). Then solution a was dripped slowly to solution b, following by keeping stirring and adding NaOH ethanol solution to adjust the pH to 6–7, reacting for 2 h in a water bath at 50 °C, then aging for 3 h at room temperature. After filtrating, repeated washing with ethanol and drying in the air, the yellow powders of RE complexes were obtained.

2.3 Preparation of the silica spheres

Monodisperse silica spheres were obtained by the classical Stöber method [27]. As the typical synthesis process, 4 ml TEOS was dropped slowly into a mixture that consisted of 60 ml ethanol, 30 ml H_2O, and 6 ml ammonia under stirring. After additional reaction for 30 min, the obtained white sol solution was centrifuged and washed with anhydrous ethanol and deionized water for several times, respectively. Finally, the samples were dried at 60 °C for 24 h in air.

2.4 Preparation of the $SiO_2@SiO_2$:$Eu(DBM)_3phen$ microspheres

The monodisperse $SiO_2@SiO_2$:$Eu(DBM)_3phen$ microspheres in a seeded growth way were synthesized in two steps. In the first step, silica seeds were prepared as above: 4 ml TEOS was rapidly dropped into a mixture that consisted of 60 ml ethanol, 30 ml H_2O, and 6 ml ammonia under stirring, and then agitated them for 30 min. In the second step, 16 ml anhydrous ethanol, 7 ml distilled water, and 2 ml ammonia were added rapidly into the above mixture under continuous stirring. After additional agitation for 15 min at room temperature, 160 mg CTAB and different ratios of $Eu(DBM)_3phen$ acetone solution (the molar composition of $Eu(DBM)_3phen$:TEOS (secondary addition) was from 1:100 to 9:100) were added slowly (the speed of dropping was about 0.2 ml/min) into the mixture which was sonicating by a sonicator. Then the mixture was sonicated for another 30 min at 600 W. Finally, some amount of TEOS was added slowly and agitated for 5 h to form the final sample. The samples were separated by centrifugation at 6000 r.p.m. for 5 min, washed with anhydrous ethanol, deionized water, and acetone for three times, respectively. The obtained samples were dried at 60 °C for 24 h in air. In order to remove residuary CTAB, the as-dried precursors were calcined at 350 °C for 3 h in nitrogen atmosphere. The heating rate was 20 °C/min.

2.5 Characterization methods

The crystal structure and phase purity of the as-prepared samples was examined by X-ray diffraction (XRD) (PANalytical B.V. X'Pert-PRO) using a XRD system with Cu-Kα radiation ($\lambda = 0.15406$ nm), working voltage of 35 kV and current of 60 mA. The morphology of the as-synthesized phosphors was investigated by using field emission scanning electron microscope (FESEM) (TESCAN MAIA3 SEM) equipped with an energy-dispersive spectrometer and transmission electron microscopy (TEM) (Zeiss Libra 200FE). The Photoluminescence (PL) excitation and PL emission spectra of rear earth complexes and $SiO_2@SiO_2$:$Eu(DBM)_3phen$ microsphere were measured at room temperature by using the luminescence spectrophotometer (Model F-4500, Hitachi) with a 150 W xenon lamp as the excitation source. Fourier transform infrared spectrum (FT-IR) spectra were measured with a Perkin–Elmer Spectrum One infrared spectrophotometer with the KBr pellet technique. Thermal gravimetric analysis and differential scanning calorimetry (TGA-DSC) data were recorded with a thermal analysis instrument (TGA/SDTA 851e, METTLER TOLEDO, Switzerland) at a heating rate of 20 °C/min in an nitrogen flow of 100 mL/min. Nitrogen adsorption–desorption isotherms were obtained at 77 K on a Micromeritics ASAP NOVA 3000 analyzer. All the measurements were performed at room temperature

3 Results and discussion

3.1 Morphology and structural analysis

The morphology and particle size distribution of the as-obtained products were investigate by SEM and TEM. Figures 1a–b show the FESEM of silica spheres synthesized by the Stöber method and core-shell $SiO_2@SiO_2$:$Eu(DBM)_3phen$ microspheres prepared by seeded growth method. As shown in Fig. 1a, the obtained silica spheres are well-dispersed and uniform with a diameter of ~ 350 nm, and their surfaces are very smooth. Similarly, the $SiO_2@SiO_2$:$Eu(DBM)_3phen$ particles formed in seeded growth way (shown in Fig. 1b) are still spherical and monodispersed, which are mainly because of the monodispersed silica spheres acting as as a growth intermediate and the secondary addition TEOS hydrolyzed into $Si(OH)_4$ depositing onto the surface of silica seeds [28]. While the average size of these particles become slightly larger than the silica spheres (as shown in Fig. 1c), and the particles are all non-aggregated with narrow size distribution (as shown in Fig. 1d) with an average size of ~ 370 nm, from which we can preliminarily conclude that a thin shell of silica which

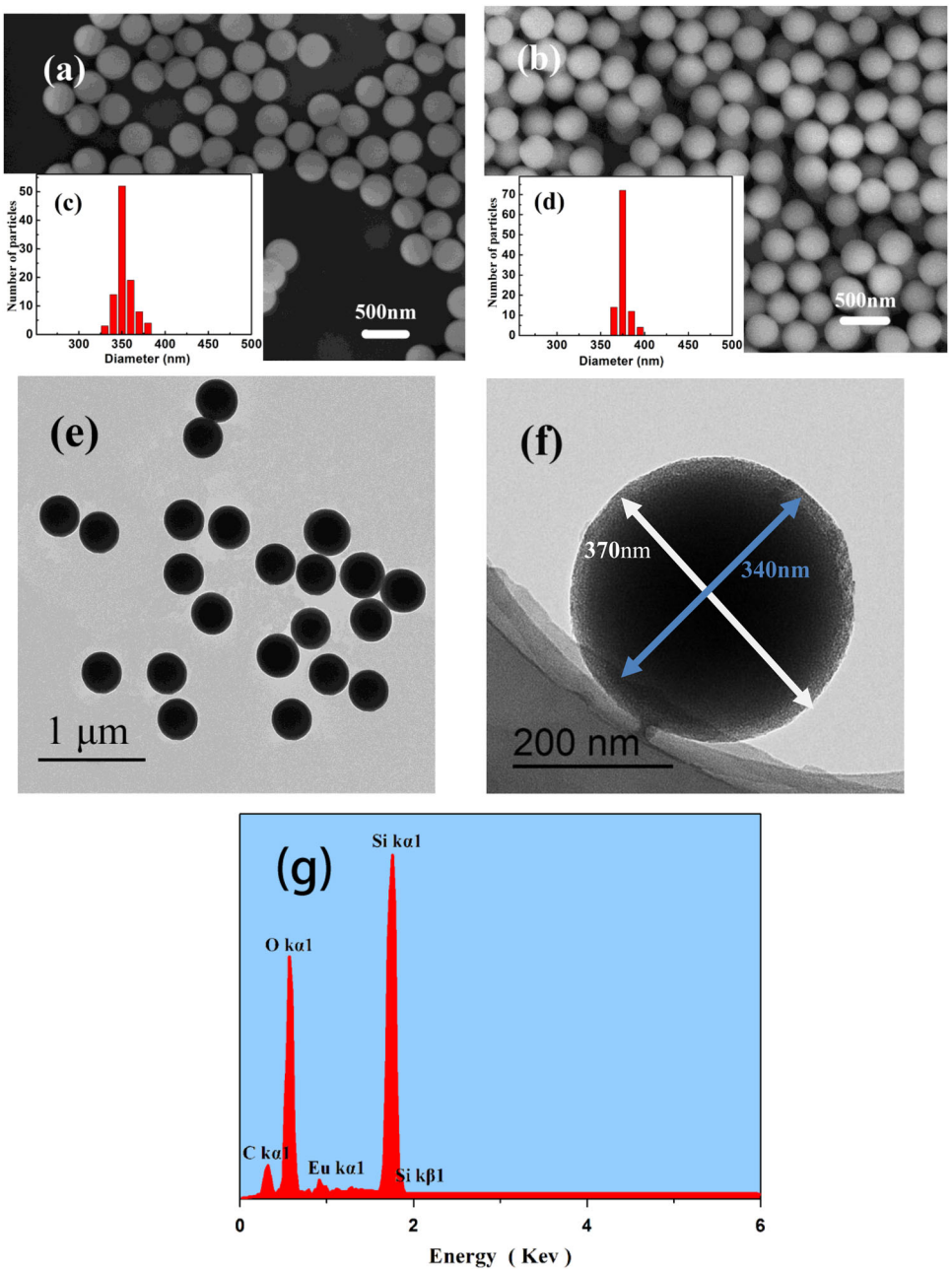

Fig. 1 The morphology and particle size distribution of the as-obtained products. **a** SEM image of silica spheres seeds; **b** SEM image of SiO_2@SiO_2:Eu $(DBM)_3$phen microspheres; **c** histograms of size distribution of silica spheres seeds; **d** histograms of size distribution of SiO_2@SiO_2:Eu$(DBM)_3$phen microspheres; **e** TEM photograph of SiO_2@SiO_2:Eu $(DBM)_3$phen microspheres in low magnification; **f** TEM image in high magnification; **g** EDX spectrum of 5.0 mol% Eu $(DBM)_3$phen-doped SiO_2@SiO_2:Eu$(DBM)_3$phen microspheres

may be doped with Eu$(DBM)_3$phen have been coated onto the surface of silica seeds by the assistance of CTAB.

To further understand the structure of SiO_2@SiO_2:Eu $(DBM)_3$phen microspheres, TEM observations were also performed. Figures 1e–f shows the TEM images of different magnification of core-shell SiO_2@SiO_2:Eu$(DBM)_3$phen microspheres prepared in seeded growth way, respectively. It can be observed from Fig. 1e and 1f that the SiO_2@SiO_2:Eu$(DBM)_3$phen particles exhibit regular sphericity and obvious core-shell structure that is composed of the black SiO_2 seeded cores with about 340 nm in diameter and gray shell with average thickness of about 15 nm. Moreover, we can find that the surface of SiO_2@SiO_2:Eu$(DBM)_3$phen microspheres are rougher than that of pure silica spheres due to poor soakage of Eu$(DBM)_3$phen fluorescent complexes on the surface of the SiO_2 seeds. TEM indicated that the outer layer of the microspheres is a thin mesoporous silica shell as the bad compatibility between the inner silica layer and the outer silica layer which may caused by the CTAB act as template agent [29].

In order to study the element composition of the final product, the as-prepared SiO_2@SiO_2:Eu$(DBM)_3$phen microspheres were analyzed by Energy-dispersive spectrometer and the results are shown in Fig. 1g. The results confirm the presence of carbon (C), silicon (Si), oxygen (O), and europium (Eu) elements in the microspheres, and there

are not any other peaks of impurity elements detected, indicating that the amorphous precursor compound has been converted to SiO_2@SiO_2:Eu(DBM)$_3$ and CTAB have been removed completely during the calcination process, which can give further support for the TEM analysis above.

The FT-IR spectra of pure earth complexes Eu(DBM)$_3$phen, pure silica spheres core-shell SiO_2@SiO_2:Eu(DBM)$_3$phen particles before and after calcination are shown in Fig. 2a–d, respectively. In the Fig. 2a, 1400–1600 cm^{-1} absorption peak are stretching vibration absorption peak of C–O, C–C, and C–N, and 3064 and 2918 cm^{-1} are the stretching vibration absorption peak of CH–CH unit of phenyl derivatives, which are all the characteristic absorption peaks of organic ligand β-diketones and phen, the peak of 1413 cm^{-1} is the stretching vibration absorption peak of C=N which comes from phen, suggesting that earth complexes Eu(DBM)$_3$phen are obtained successfully. For the Fig. 2b–d, there are the typical absorption bands of Si–O–Si (1105 cm^{-1}, 805 cm^{-1}), Si–OH (470 cm^{-1}) and –OH vibration peak near 3430 and 1610 cm^{-1}. Meanwhile, compared with Fig. 2d, it is easy to find in Fig. 2b and c that weak vibration peaks appear in 1400–1600 cm^{-1} which are C=O, C=C, C=N stretching vibration peaks of β-diketone and phen, and the peaks of 2925 cm^{-1} are the stretching vibration absorption peak of CH–CH unit of phenyl derivatives and CTAB, indicating that the surface of silica seeds are covered with a layer of SiO_2 shell which is doped with Eu(DBM)$_3$phen successfully. However, there are few differences between Fig. 2b and 2c, as the content of CTAB is low and the similarities of FT-IR spectra between CTAB and β-diketones. Through the FT-IR spectra of Fig. 2a–d, it can be indirectly indicated that the microspheres which are doped with RE complexes were obtained.

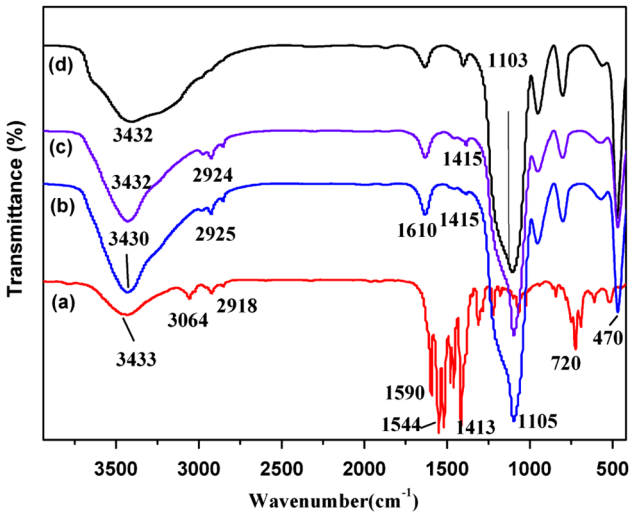

Fig. 2 FT-IR spectra of pure earth complexes Eu(DBM)$_3$phen **a**, 5.0 mol% Eu(DBM)$_3$phen-doped core-shell SiO_2@SiO_2:Eu(DBM)$_3$phen particles before **b** and after calcination **c**, and pure silica spheres **d**

Figure 3 shows the X-ray diffraction patterns of the pure RE complexes, core-shell SiO_2@SiO_2:Eu(DBM)$_3$phen particles formed in seed growth way and pure silica spheres prepared via base-catalyzed Stöber method, respectively. The peak positions of the Eu(DBM)$_3$Phen well match with the literatures [30, 31], the characteristic peaks of the complexes lie at 2θ ~8.2°, 8.7°, and 17.4° positions in which the first two are mainly due to Eu^{3+} ions and the later one is the new peak which may be generated due to increased cell size. For pure silica spheres and core-shell SiO_2@ SiO_2:Eu(DBM)$_3$phen particles, the position of band center are around 23°, which is the amorphous SiO_2 characteristic pattern. Careful view shows that there are some weak peaks (marked with *red circles* in Fig. 3b) appeared in the XRD of SiO_2@SiO_2:Eu(DBM)$_3$phen particles, which are attributed to RE complexes as shown in Fig. 3a, indicating that Eu(DBM)$_3$phen have been incorporates into SiO_2 shell successfully. The low-angle XRD pattern of SiO_2@SiO_2:Eu(DBM)$_3$phen microspheres have been shown in Fig. 3d, the microspheres show a tense peak at 2θ =1.89°, revealing that the SiO_2@SiO_2:Eu(DBM)$_3$phen microspheres have ordered hexagonal mesopore symmetry, which is due to the mesopore channels are perpendicular to the surface of silica seeds, ethanol can lower the hydrolysis

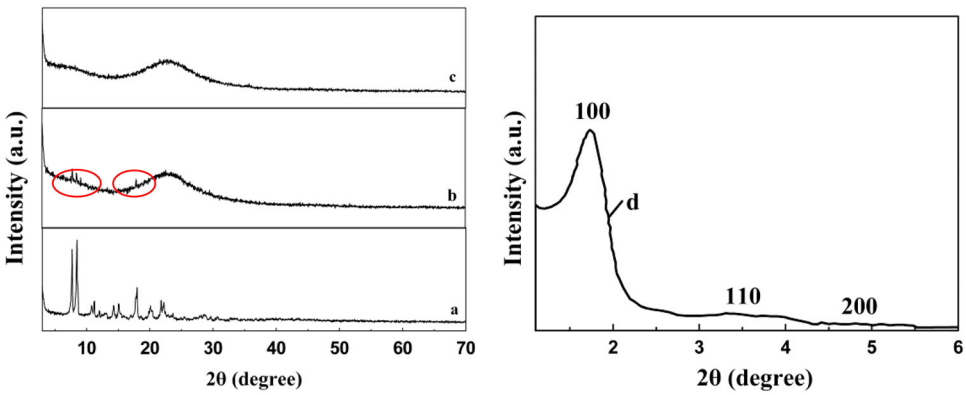

Fig. 3 XRD patterns of the pure RE complexes **a**, 5.0 mol% Eu(DBM)$_3$phen-doped core-shell SiO_2@SiO_2: Eu(DBM)$_3$phen particles **b**, pure silica spheres **c** and low-angle XRD pattern of SiO_2@SiO_2:Eu(DBM)$_3$phen microspheres **d**

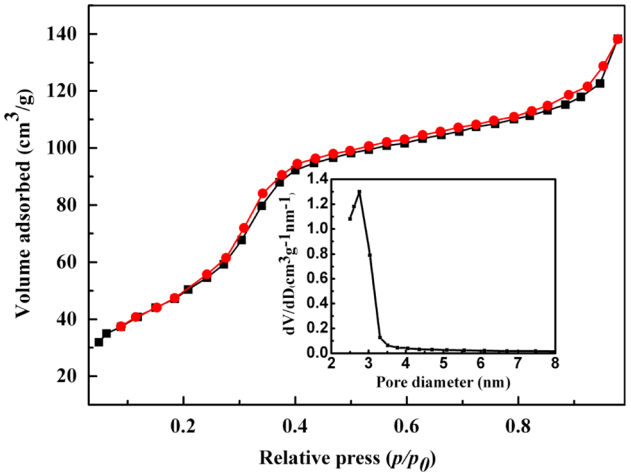

Fig. 4 N_2 adsorption-desorption isotherms and mesopore size distribtuion (the inset) of the synthesized SiO_2@SiO_2:Eu(DBM)$_3$phen microspheres. The adsorption branch is shown in *black color* and the desorption branch in *red color*

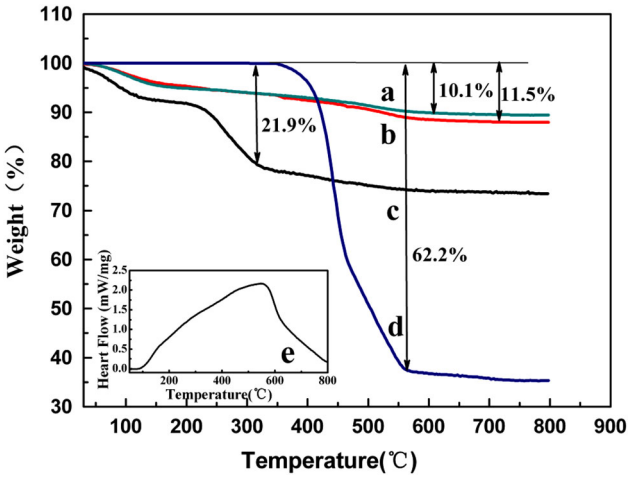

Fig. 5 TGA curves of pure silica spheres **a**, 5.0 mol% Eu(DBM)$_3$phen-doped core-shell SiO_2@SiO_2:Eu(DBM)$_3$phen particles (after calcination) **b**, 5.0 mol% Eu(DBM)$_3$phen-doped core-shell SiO_2@SiO_2:Eu(DBM)$_3$phen particles (before calcination) **c** and pure Eu(DBM)$_3$phen **d**; Inset is the corresponding DSC curve of SiO_2@-SiO_2:Eu(DBM)$_3$phen particles after calcination **e**

and condensation rate of TEOS and favor the coating and curving [32].

The nitrogen adsorption-desorption isotherms of SiO_2@SiO_2:Eu(DBM)$_3$phen microspheres and the corresponding pore size distribution analyses are shown in Fig. 4. The isotherms exhibit IV-type curve with an obvious hysteresis loop, indicating the mesoporous characteristics of the silica shell. The BET surface area and total pore volume are calculated to be 269 m^2/g and 0.274 cm^3/g, respectively. The mesopore size distribution exhibits a sharp peak at the mean value of 2.9 nm (Fig. 4, inset), indicating the uniform mesopore of the silica shell.

The thermogravimetric analysis (TGA) curves of pure silica spheres, pure Eu(DBM)$_3$phen, SiO_2@SiO_2:Eu(DBM)$_3$phen particles before and after calcination are shown in Fig. 5. And the corresponding DSC curve of SiO_2@SiO_2:Eu(DBM)$_3$phen after calcination is shown in Fig. 5e. The products were heated from 30 to 800 °C with the heating rate of 20 °C/min under N_2 atmosphere. For pure RE complexes Eu(DBM)$_3$phen, It started to decompose at about 380 °C and the mass loss increased to about 62.2% when the temperature rose to 600 °C(in Fig. 5d), which are mainly resulted from the release of H_2O, CO_2, NO_2, NH_3 gases from the thermal decomposition of Eu(DBM)$_3$Phen. For SiO_2@SiO_2:Eu(DBM)$_3$phen particles after calcination (in Fig. 5b), a small weight loss from 30 to 150 °C with endothermic peak was observed, due to the loss of the adsorbed water molecules. A large weight loss from 250 to 600 °C with exothermic peak attributed to the condensation among silanol groups was observed (the same as pure silica spheres in Fig. 5a) and the decomposition of Eu(DBM)$_3$phen. Meanwhile, a large weight loss from 190 to 300 °C appears in Fig. 5c, which caused by the decomposition of CTAB, but it didn't appear in Fig. 5b, manifesting that the residuary CTAB have been removed completely after calcination. In addition, It's easy to find that the thermal stability of the RE complexes has been greatly improved by incorporating into SiO_2 matrix. It may be caused by weak interactions between lanthanide complexes and the SiO_2 matrix, such as van der Waals' contacts, hydrogen bonding, or electrostatic forces [33, 34]. And Fig. 5 gives a basis for the calcining process to remove the surfactant CTAB.

3.2 Formation process

On the basis of above experimental results, a possible formation process for the SiO_2@SiO_2:Eu(DBM)$_3$phen composite microspheres was proposed and shown in Fig. 6. Firstly, monodisperse silica spheres were formed via base-catalyzed hydrolysis of TEOS, and obviously there should be many hydroxyl groups with high activity on the surface of silica seeds. Secondly, as the surfactant, the hydrophilic end (marked with *blue part*) of CTAB connected with the surface of silica microspheres, and its hydrophobic end (marked with *red part*) connected with Eu(DBM)$_3$phen. With the secondary addition of TEOS and the occurrence of further hydrolysis reaction, the generated SiO_2 along with RE complexes depositing on the surface of silica seeds and forming a mesoporous silica layer [35] which contains flourescent Eu(DBM)$_3$phen. Finally, the residuary CTAB is removed by a calcining process and the final products SiO_2@SiO_2:Eu(DBM)$_3$phen composite microspheres were obtained.

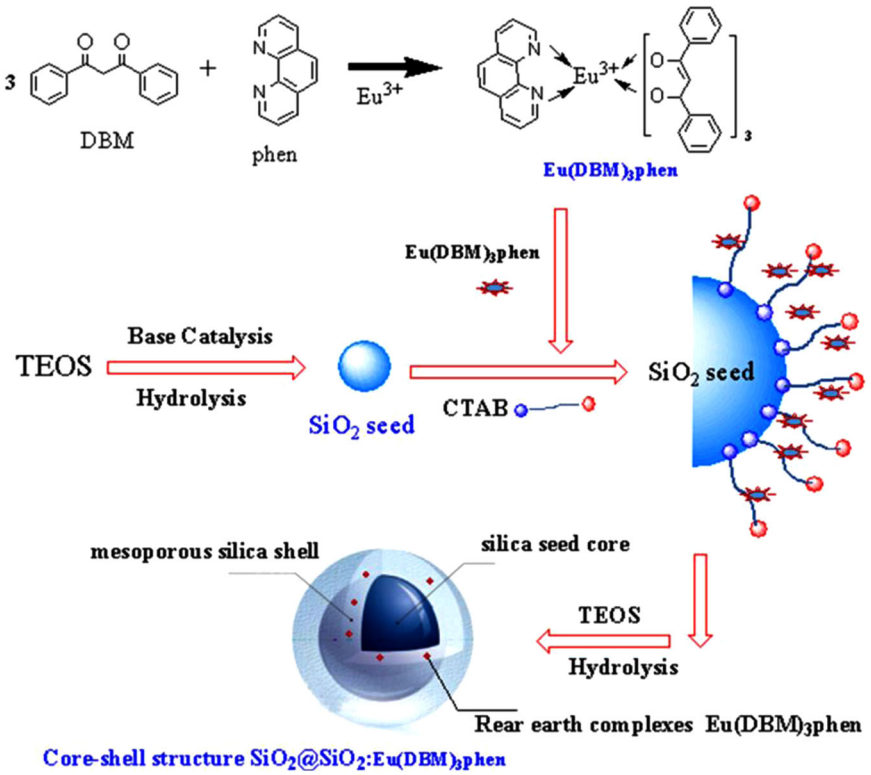

Fig. 6 The formation mechanism of $SiO_2@SiO_2$: Eu $(DBM)_3$phen microspheres

3.3 Luminescence properties

The photoluminesence properties of the as-obtained products are shown in Fig. 7. Figure 7a shows the excitation spectra of the pure Eu$(DBM)_3$phen, core-shell $SiO_2@SiO_2$: Eu$(DBM)_3$phen microspheres before and after calcination at 610 nm. It can be clearly observed from Fig. 7a that all excitation spectrums exhibit a very broad band ranging from 250 to 500 nm with the maximum excitation wavelength centered at about 405 nm which belongs to Eu^{3+} ion f-f absorption transition from $^7F_0 \rightarrow {}^5L_6$ [36]. Compared with the pure RE complexes, the maximum excitation wavelength of core-shell $SiO_2@SiO_2$:Eu$(DBM)_3$phen microspheres shows a small blue shift changing from 403 to 410 nm, implying that different compositions may exist between the two samples caused by the silica matrix. In addition, there is little difference between the excitation spectra of $SiO_2@SiO_2$:Eu$(DBM)_3$phen microspheres before and after calcination, indicating no thermal decomposition of Eu$(DBM)_3$Phen in the calcining process.

As is shown in Fig. 7b, compared with silica spheres doped with Eu^{3+} (prepared as report [17]), the core-shell $SiO_2@SiO_2$:Eu$(DBM)_3$phen microspheres before and after calcination show much higher luminous intensity. The insets in Fig.7b are photographs of the 2 mol% Eu^{3+}-doped SiO_2:Eu^{3+} and 2 mol% Eu$(DBM)_3$phen-doped core-shell $SiO_2@SiO_2$:Eu$(DBM)_3$phen microspheres under UV light irradiation ($\lambda_{ex} = 365$ nm), it can be observed that the core-shell $SiO_2@SiO_2$:Eu$(DBM)_3$phen microspheres emit strong red PL upon irradiation with ultraviolet light while the SiO_2:Eu^{3+} microspheres emit almost no light, which can be proved further by the emission spectra ($\lambda_{ex} = 395$ nm) of Fig. 7b1–b2. It shows that the peak positions and spectral shapes of emission spectra are not influenced by replacing Eu^{3+} ion with Eu$(DBM)_3$phen, but the luminous intensity increase a lot, which is caused by the influence of orgnic ligands (the mechanism is shown in Fig. 7c): the DBM and phen should work as a "antenna" for the Eu^{3+}, augmenting the number of photons converted into visible region [20]. Therefore, The RE complexes show much better luminous performance than the RE ions. And the luminous intensity of $SiO_2@SiO_2$:Eu$(DBM)_3$phen microspheres before calcination is higher than the microspheres of after calcination (as shown in Fig. 7b3), which may caused by the"Fluorescence protector" effect provided by CTAB [37].

In order to investigate the effect of the dopant concentration on PL intensities, the concentrations of Eu $(DBM)_3$phen dopants were varied from 1 to 9 mol%. Figure 7d shows the emission spectra of $SiO_2@SiO_2$:Eu $(DBM)_3$phen with the RE complexes dopant concentration of 1.0, 1.5, 2.0, 3.0, 5.0, 7.0, and 9.0 mol%, respectively. These spectral shapes are almost same irrespective of the RE complexes concentration. Under the excitation of 405 nm, the emission spectrum consists of the $^5D_0 \rightarrow {}^7F_J$ ($J = 0$, 1, 2, 3) (577, 595, 610, and 648 nm) transition of the Eu^{3+}

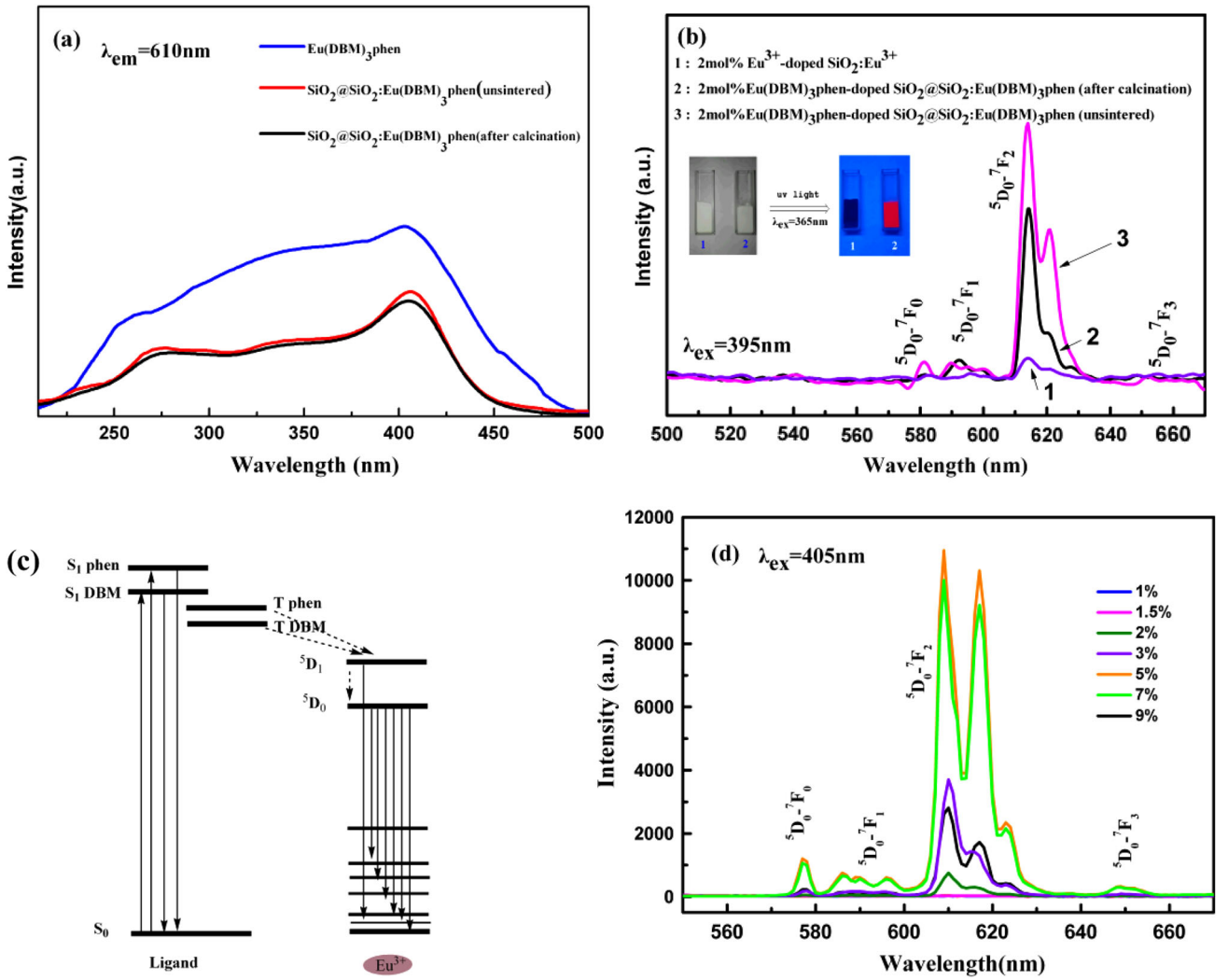

Fig. 7 The photoluminesence properties of the as-obtained products. **a** excitation spectra of pure $Eu(DBM)_3Phen$ complexes, core-shell $SiO_2@SiO_2$:$Eu(DBM)_3$phen microspheres before and after calcination; **b** emission spectra of 2.0 mol% Eu^{3+}-doped silica spheres (1), 2.0 mol% $Eu(DBM)_3$phen-doped $SiO_2@SiO_2$:$Eu(DBM)_3$phen microspheres before (2) and after calcination (3); **c** Schematic representation of photophysical processes of $Eu(DBM)_3$phen; **d** emission spectra of $SiO_2@SiO_2$:$Eu(DBM)_3$phen microspheres with different RE complexes concentration

ions. The strongest emission peaking at 610 nm arises from the electric-dipole allowed $^5D_0 \rightarrow {}^7F_2$ transition of Eu^{3+} ions, which are caused by the lack of inversion symmetry at Eu^{3+} ions site [38]. The positions of the luminescence peaks in emission spectrum do not change significantly with increasing of the RE complexes concentration, but the intensity of the hypersensitive $^5D_0 \rightarrow {}^7F_2$ peak shows a linear increase with the concentration of RE complexes increasing about to 7 mol% where it starts to bend towards an asymptotic behavior, then decreases with more addition of RE complexes, which is regarded as the typical concentration quenching effect [39], and it is due to the interface effects of silicon hydroxyls and space steric hindrance that hinder the energy transfer between the activator ions.

4 Conclusions

Core-shell structural $SiO_2@SiO_2$:$Eu(DBM)_3$phen microspheres have been successfully prepared via a seeded growth method which can enhance the fluorescent signal and increase the photostability by encapsulating the hydrophobic europium complexes into hydrophilic silica shell by means of surfactant CTAB. The samples are well dispersed and uniform spheres with the diameter of ~ 370 nm, which include the core diameter of ~ 340 nm and the shell thickness of ~ 15 nm. The formation process of $SiO_2@SiO_2$:$Eu(DBM)_3$phen microspheres is proposed in detail. The as-obtained microspheres show a much stronger red emission corresponding to the $^5D_0 \rightarrow {}^7F_2$ transition of the Eu^{3+} ions under ultraviolet light excitation $\lambda_{ex} = 405$

nm compared with SiO_2:Eu^{3+}, and the PL intensity for the 450–750 nm emission increases with increasing of Eu $(DBM)_3$phen's concentration and reaches the maximum when the concentration of Eu$(DBM)_3$phen is 7.0 mol%. This method is simple and can reduce the usage of expensive RE ions. The as-obtained microspheres may present potential applications in the fields of optoelectronic devices, bioimaging, medical diagnosis, and study on the structure of functional composites.

Acknowledgements This work was supported by the Sichuan Science and Technology Support Project in China (2013GZX0164), the National 863 Project (2015AA034004) and the Mianyang city science and technology plan projects (14G-03-7).

Compliance with ethical standards

Conflict of interest The authors declare that they have no competing interests.

References

1. Yuan B, Song Y, Sheng Y, Zheng K, Huo Q, Xu X, Zou H (2014) Luminescence properties and energy transfer of Ca2Mg0.5Al-Si1.5O7:Ce3+, Eu2+ phosphors for UV-excited white LEDs. Powder Technol 253:803–808
2. Bünzli J-CG (2010) Lanthanide luminescence for biomedical analyses and imaging. Chem Rev 110(5):2729–2755
3. Miao G, Chen X, Mao C, Li X, Li Y, Lin C (2013) Synthesis and characterization of europium-containing luminescent bioactive glasses and evaluation of in vitro bioactivity and cytotoxicity. J Sol-Gel Sci Technol 69(2):250–259
4. Comby S, Surender EM, Kotova O, Truman LK, Molloy JK, Gunnlaugsson T (2014) Lanthanide-functionalized nanoparticles as MRI and luminescent probes for sensing and/or imaging applications. Inorg Chem 53(4):1867–1879
5. Li Q, Lin J, Wu J, Lan Z, Wang Y, Peng F, Huang M (2013) Improving photovoltaic performance of dye-sensitized solar cell by downshift luminescence and p-doping effect of Gd2O3:Sm3+. J Lumin 134:59–62
6. Li H, Sheng Y, Zhang H, Xue J, Zheng K, Huo Q, Zou H (2011) Synthesis and luminescent properties of TiO2:Eu3+ nanotubes. Powder Technol 212(2):372–377
7. Zhang Q, Sheng Y, Zheng K, Zou H (2015) New kinds of hybrid materials containing covalently bonded Tb3+ (Eu3+) complexes organically modified titania and alumina network via sol-gel process. J Sol-Gel Sci Technol 77(1):152–159
8. Hu Y, Zhuang W, Ye H, Zhang S, Fang Y, Huang X (2005) Preparation and luminescent properties of (Ca1-x,Srx)S:Eu2+ red-emitting phosphor for white LED. J Lumin 111(3):139–145
9. Hlásek T, Polák V, Rubešová K, Jakeš V, Nekvindová P, Jankovský O, Mikolášová D, Oswald J (2016) Sol-gel-derived planar waveguides of Er3+:Yb3Al5O12 prepared by a polyvinylpyrrolidone-based method. J Sol-Gel Sci Technol 80 (2):531–537
10. Wang Q, Zhu G, Xin S, Ding X, Xu J, Wang Y, Wang Y (2015) A blue-emitting Sc silicate phosphor for ultraviolet excited light-emitting diodes. Phys Chem Chem Phys 17(41):27292–27299
11. Cheng Q, Kang M, Wang J, Zhang P, Sun R, Song L (2015) Low temperature microwave solid-state synthesis of CaCO3: Eu3+, K + phosphors. Adv Powder Technol 26(3):848–852
12. Zhao D, Qin W, Zhang J, Wu C, Qin G, De G, Zhang J, Lü S (2005) Modified spontaneous emission of europium complex nanoclusters embedded in colloidal silica spheres. Chem Phys Lett 403(1-3):129–134
13. Ansari AA, Hasan TN, Syed NA, Labis JP, Parchur AK, Shafi G, Alshatwi AA (2013) In-vitro cyto-toxicity, geno-toxicity, and bio-imaging evaluation of one-pot synthesized luminescent functionalized mesoporous silica@Eu(OH)3 core-shell microspheres. Nanomedicine 9(8):1328–1335
14. Wang G, Zou H, Gong L, Shi Z, Xu X, Sheng Y (2014) Synthesis and luminescent properties of monodisperse core-shell structured SiO2@Lu2O3:Eu3+ microspheres. Powder Technol 258:174–179
15. Wang H, Yu M, Lin CK, Liu XM, Lin J (2007) Synthesis and luminescence properties of monodisperse spherical Y2O3:Eu3+ @SiO2 particles with core-shell structure. J Phys Chem C 111 (30):11223–11230
16. Fu ZF, Li WX, Bai J, Bao JR, Cao XF, Zheng YS (2016) Synthesis, characterization and luminescence of europium perchlorate with MABA-Si complex and coating structure SiO2 @Eu (MABA-Si) luminescence nanoparticles. Lumin: J Biol Chemical Lumin. doi:10.1002/bio.3182
17. Gong L, Zou H, Wang G, Sun Y, Huo Q, Xu X, Sheng Y (2014) Synthesis and luminescence properties of monodisperse SiO2@-SiO2:Eu3+ microspheres. Opt Mater 37:583–588
18. Liu Y-M, Wu Y-C (2012) Synthesis of europium-doped silica microspheres using the sol-gel microencapsulation method. J Sol-Gel Sci Technol 63(1):36–44
19. de Dood MJ, Berkhout B, van Kats CM, Polman A, van Blaaderen A (2002) Acid-based synthesis of monodisperse rare-earth-doped colloidal SiO2 spheres. Chem Mater 14(7):2849–2853
20. Feng J, Zhang H (2013) Hybrid materials based on lanthanide organic complexes: a review. Chem Soc Rev 42(1):387–410
21. Daojun Zhang XW, Qiao Zhen-an, Tang D, Liu Y, Huo Q (2010) Synthesis and characterization of novel lanthanide (III) complexes-functionalized mesoporous silica nanoparticles as fluorescent nanomaterials. J Phys Chem C 114(29):12505–12510
22. Guanshi Q, Lin H (2004) Fabrication and luminescence of rare earth complex/SiO2 hybrid nanospheres. J Rare Earths 22(1):49
23. Zhao D, Qin W, Zhang J, De G, Zhang J (2005) Improved thermal stability of europium complex nanoclusters embedded in silica colloidal spheres. Chem Lett 34(3):366–367
24. Zhao D, Qin W, Wu C, Qin G, Zhang J, Lü S (2004) Laser selective spectroscopy of europium complex embedded in colloidal silica spheres. Chem Phys Lett 388(4-6):400–405
25. Yu M, Chen G, Liu J, Tang B, Huang W (2013) Preparation and characteristics of core-shell structure Eu(DBM)3Phen@SiO2 micro-sphere. J Mater Sci Technol 29(9):801–805
26. Melby LR, Rose NJ, Abramson E, Caris JC (1964) Synthesis and fluorescence of some trivalent lanthanide complexes. J Am Chem Soc 86(23):5117–5125
27. Stöber W, Fink A, Bohn E (1968) Controlled growth of monodisperse silica spheres in the micron size range. J Colloid Interface Sci 26(1):62–69
28. Chen SL, Peng D, Yang GH, Yang JJ (1996) Characteristic aspects of formation of new particles during the growth of monosize silica seeds. J Colloid Interface Sci 180(1):237–241
29. Zhao S, Zhang Y, Zhou Y, Sheng X, Zhang C, Zhang M, Fang J (2016) One-step synthesis of core-shell structured mesoporous silica spheres templated by protic ionic liquid and CTAB. Mater Lett 178:35–38
30. Singh AK, Singh SK, Mishra H, Prakash R, Rai SB (2010) Structural, Thermal, and Fluorescence Properties of Eu (DBM)

3Phen x Complex Doped in PMMA. J Phys Chem B 114 (41):13042–13051
31. Liu HG, Park S, Jang K, Zhang W, Seo H-J, Lee Y-I (2003) Different photoluminescent properties of binary and ternary europium chelates doped in PMMA. Mater Chem Phys 82 (1):84–92
32. Deng Y, Qi D, Deng C, Zhang X, Zhao D (2008) Superparamagnetic high-magnetization microspheres with an Fe3O4@ SiO2 core and perpendicularly aligned mesoporous SiO2 shell for removal of microcystins. J Am Chem Soc 130(1):28–29
33. Fu L, Ferreira RAS, Nobre SS, Carlos LD, Rocha J (2007) In situ synthesis of lanthanide complex in urea cross-linked organic/inorganic di-ureasil hybrids via carboxylic acid solvolysis. J Lumin 122-123:265–267
34. Sun LN, Zhang HJ, Meng QG, Liu FY, Fu LS (2005) Near-infrared luminescent hybrid materials doped with lanthanide (Ln) complexes (Ln=Nd, Yb) and their possible laser application. J Phys Chem B 109(13):6174–6182
35. Gorelikov I, Matsuura N (2008) Single-step coating of mesoporous silica on Cetyltrimethyl ammonium bromide-capped nanoparticles. Nano Lett 8(1):369–373
36. Zhang HJ, Fu LS, Wang SB, Meng QG, Yang KY, Ni JZ (1999) Luminescence characteristics of europium and terbium complexes with 1,10-phenanthroline in-situ synthesized in a silica matrix bya two-step sol-gel progress. Mater Lett 38(4):260–264
37. Wang C, Zhang R, Möhwald H (2010) Micelles as "Fluorescence Protector" for an Europium complex in microcapsules. Langmuir 26(14):11987–11990
38. Zhang H, Sheng Y, Zhou X, Song Y, Shi Z, Xu X, Zou H (2015) Novel 3D flower-like TiO2:Eu3+ hierarchitectures: Hydrothermal synthesis and luminescent properties. Powder Technol 274:193–198
39. Moretti E, Bellotto L, Basile M, Malba C, Enrichi F, Benedetti A, Polizzi S (2013) Investigation on the effect of Tb(dbm)3phen on the luminescent properties of Eu(dbm)3phen-containing mesoporous silica nanoparticles. Mater Chem Phys 142(1):445–452